

Pellicle induced Aberration and Apodization in Hyper NA Optical Lithography

Karsten Bubke^{*1}, Benjamin Alles², Eric Cotte¹, Martin Sczyrba¹, Christophe Pierrat¹

¹Advanced Mask Technology Center GmbH & Co. KG, Raehnitzer Allee 9, D-01109 Dresden, Germany

²Technische Universität München, Boltzmannstr. 3, D-85748 Garching, Germany

ABSTRACT

In 193nm optical lithography, immersion technology will enable numerical apertures much greater than 1.0. Furthermore, polarized light is likely to be applied, enhancing the imaging properties of structures with dimensions near the resolution limit. As a result, the consequences of extreme oblique angle illumination as well as polarization effects need to be carefully evaluated for all elements of the lithographic process. This paper explores the aberrations and apodization induced by the pellicle film in hyper NA lithography.

In a first step, the angle and polarization-dependent phase errors of a perfectly flat pellicle are investigated and discussed for varying thicknesses. It will be shown that for NAs greater than 1.0 the pellicle induces higher order spherical aberrations which can be in the range of today's scanner lens specifications. Also, the impact of polarization-dependent apodization will be discussed.

In a second step, the analysis is extended to the case of a non-flat pellicle due to a given frame bow. Under these conditions, the phase and transmission error is not radially symmetric and, furthermore, is field dependent. It will be discussed under which conditions this effect can lead to a significant pellicle-induced CD signature over the entire image field.

Keywords: Pellicle, Hyper NA Lithography, Aberration, Apodization, CD uniformity

1. INTRODUCTION

Immersion technology enables NAs greater than 1.0. Whereas for water as an immersion liquid the NA of scanners is limited to 1.35, research on new immersion liquids and new lens materials with higher refractive index is underway. This might allow the extension of immersion lithography to NAs up to 1.65 or even larger. At these high angles, polarized illumination will most likely be used to enhance imaging properties. The application of polarized light requires the preservation of the desirable polarization state throughout the entire optical system [1-4]. As a result, all elements of the projection system need to be reevaluated with respect to their influence not only on wavefront but also on polarization properties. This applies particularly to the different elements of the photomask.

A prominent example for this reevaluation is mask birefringence. For unpolarized illumination the birefringence of the reticle is not an issue. Using polarized light, mask birefringence can alter the polarization of the illumination which in return causes CD errors[1]. Investigations showed that birefringence values lower than 2-5 nm/cm are necessary to prevent any influence of mask birefringence on CD for NAs up to 1.35 [1,5].

Polarization and phase effects of the structured surface of the mask are an active field of research [6]. It has been shown in a number of publications that mask topography can have a significant influence on the lithographic performance, ranging from CD errors to image degradation.

A mask element which, to our knowledge, has not been looked at in the context of Hyper NA lithography is the pellicle. The influence of off axis transmission of pellicles has been discussed, for example, in [14]. For 157nm lithography, a considerable amount of research was dedicated to the introduction of hard pellicles, in particular to their influence on aberrations [7]. The much thinner membrane used in 193 nm lithography was not considered to be an issue so far. However, at NAs of 1.35 or even larger, the angle of incidence on the pellicle can reach values up to 20-25°.

* karsten.bubke@amtc-dresden.com, phone +49 351 4048 377, fax +49 351 4048 9377

This might introduce not only a considerable amount of aberration levels but also apodization. Furthermore, polarization properties like retardation and diattenuation and their influence on the lithographic performance need to be examined. Some first experimental results on polarization dependent transmission were presented in [8].

In this paper we investigate the transmission properties of the pellicle membrane when exposed under large oblique angles. Also, we look at the influence of thickness variations of the pellicle membrane as well as film shape due to a non perfect pellicle frame.

2. TRANSMISSION THROUGH PELLICLE MEMBRANE

A typical geometry of a pellicle routinely used in 193nm lithography is shown in Fig. 1. A thin polymer membrane is suspended over an aluminum frame, which is glued to the surface of the reticle. It has been shown in a number of publications that the attachment of an initially distorted pellicle frame can cause significant in-plane and out-of plane distortions [12, 13]. However, in this paper we are mainly interested in the optical properties of the pellicle film.

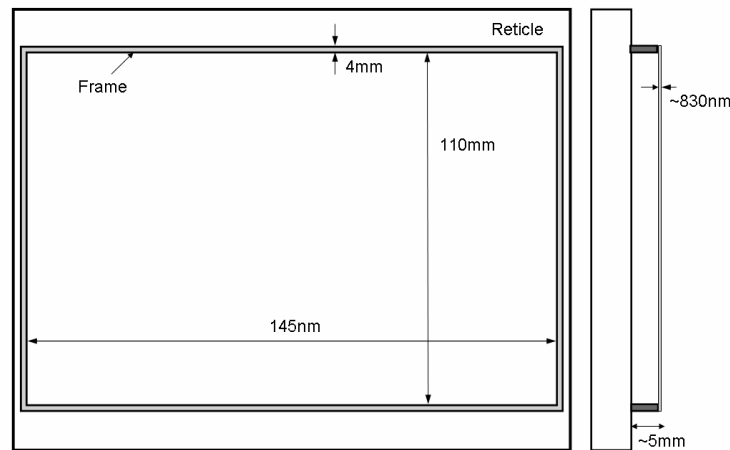


Figure 1: Typical dimensions of a pellicle mounted to a reticle.

The transmission of the pellicle membrane depends on the film thickness, the wavelength, the incident angle and the polarization of light. For maximum transmission at normal incidence, the film thickness is chosen to be an integer of half the wavelength in the film. Pellicle films used in 193nm lithography do not usually have an antireflective coating. The optical properties of the membrane can change significantly with cumulated exposure [9]. However, in our analysis we assume a homogeneous film with a nominal thickness of $h=828\text{nm}$ and a refractive index of $n=1.4$ which is optimized for normal transmission at 193.3 nm wavelength. The material is assumed to have no attenuation at the actinic wavelength. Furthermore, in our analysis multiple reflections between pellicle and mask surface are neglected.

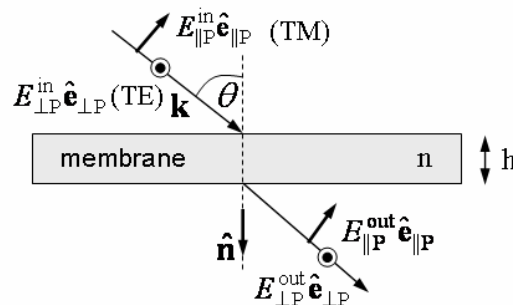


Figure 2: Transmission through pellicle membrane – definition of relevant parameter.

The angle and polarization dependent transmission through the pellicle film can be described by the theory of dielectric films [10]. As illustrated in Fig. 2, an incoming plane wave can be decomposed into two components, one having its electric field vector perpendicular to the plane of incidence (TE - denoted by the symbol \perp) and one with an electric field vector located in the plane of incidence (TM - denoted by the symbol \parallel). For arbitrary directions of the wave vector \mathbf{k} and the surface normal of the pellicle film \mathbf{n} , the directions of the field components are given by,

$$\hat{\mathbf{e}}_{\perp P} = \frac{\mathbf{n} \times \mathbf{k}}{|\mathbf{n} \times \mathbf{k}|} \text{ and } \hat{\mathbf{e}}_{\parallel P} = \frac{\hat{\mathbf{e}}_{\perp P} \times \mathbf{k}}{|\hat{\mathbf{e}}_{\perp P} \times \mathbf{k}|}. \quad (1)$$

With the naming convention introduced in Fig. 2, the impact of the pellicle on the polarization state can be written as,

$$\begin{pmatrix} E_{\parallel P}^{\text{out}} \\ E_{\perp P}^{\text{out}} \end{pmatrix} = \mathbf{F} \cdot \begin{pmatrix} E_{\parallel P}^{\text{in}} \\ E_{\perp P}^{\text{in}} \end{pmatrix}, \text{ with } \mathbf{F} = \begin{bmatrix} A_{\parallel}(\vartheta, h) \exp(i\varphi_{\parallel}(\vartheta, h)) & 0 \\ 0 & A_{\perp}(\vartheta, h) \exp(i\varphi_{\perp}(\vartheta, h)) \end{bmatrix}. \quad (2)$$

A and ϕ represent the attenuation and phase introduced by the pellicle membrane. In the expressions for the phase we additionally subtracted a phase corresponding to the optical path when no pellicle is present. The actual analytical expressions for thin film transmission can be found in standard textbooks [10] and are not reproduced here.

In Fig. 3, the calculated normalized transmission and phase introduced by a pellicle with parameters as stated above are plotted for varying angles of incidence. The maximum angle of a plane wave captured by the entrance pupil of a scanner lens with magnification factor 0.25 is given by $\vartheta_{\text{max}} = \text{asin}(\text{NA}/4)$; respective angles are given in Tab. 1. For NAs smaller than 1, the transmission error is relatively small. However, the pellicle induced apodization grows significantly for NAs larger than 1.2 and becomes polarization dependent. The pellicle induced phase can reach values up to 25° for an NA of 1.35.

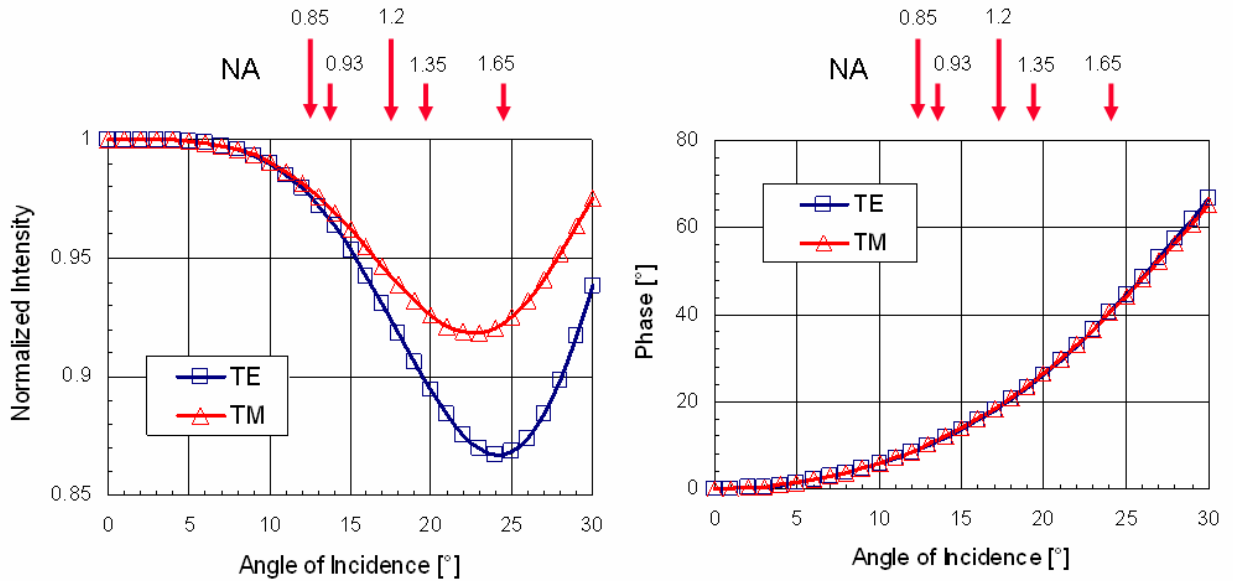


Figure 3: Normalized transmission $|A_{\perp}|^2$ (TE) and $|A_{\parallel}|^2$ (TM) as well as phase of a pellicle film with thickness $h=828\text{nm}$ and refractive index $n=1.4$ at a wavelength of 193.3nm ; also given are the maximum angles of incidence on the pellicle for a given NA of the scanner lens.

NA	0.75	0.85	0.93	1.2	1.35	1.65
$\vartheta_{\text{max}} (^{\circ})$	10.8	12.3	13.4	17.5	19.7	24.4

Table 1: Maximum angle of incidence captured by the entrance pupil of the lens for different NAs.

In this paper we are interested in pellicle induced aberrations and apodization and their dependence on polarization. It is therefore convenient to separate the angle dependent transmission properties of the pellicle film into scalar transmission and diattenuation. In a similar manner, the pellicle induced phase can be characterized by a scalar phase and retardance. The scalar transmission T and the phase ϕ are defined as,

$$T = \frac{1}{2} [A_{\parallel}^2(\vartheta, h) + A_{\perp}^2(\vartheta, h)], \quad \phi = \frac{1}{2} [\phi_{\parallel}(\vartheta, h) + \phi_{\perp}(\vartheta, h)]. \quad (3)$$

Diattenuation D is a measure for different attenuation between TE and TM and can be written as,

$$D = \frac{A_{\perp}^2(\vartheta, h) - A_{\parallel}^2(\vartheta, h)}{A_{\perp}^2(\vartheta, h) + A_{\parallel}^2(\vartheta, h)}. \quad (4)$$

Finally, the retardance $\Delta\phi$ is defined as the difference in induced phase for the different polarization states,

$$\Delta\phi = \phi_{\perp}(\vartheta, h) - \phi_{\parallel}(\vartheta, h). \quad (5)$$

In the following, these quantities and their dependence on film thickness will be discussed separately.

Scalar Transmission

Fig. 4 shows the scalar transmission as defined in Eq. 3 for various thicknesses of the pellicle membrane. As was indicated in Fig. 3, for angles larger than 10° a significant apodization can be observed. This leads to a transmission loss of about 10% at the outer rim of the pupil for $NA=1.35$. The radial apodization observed here might have implications on OPC; an example is given in a subsequent section. However, similar effects are given by the obliquity factor or the coupling into the resist on wafer. More interesting is the change of transmission with pellicle thickness which can lead to a dose variation when the wafer is exposed.

At normal incidence, the loss in transmission is smaller than 1% for a thickness variation of $\pm 5\text{nm}$. However, the change in transmission for larger angles becomes significant. This is shown in the right plot of Fig. 4. Here, the change in transmission is plotted at a pupil coordinate $0.9NA$ for different NAs, and hence refers to the apodized intensity at a certain angle. The pellicle-induced transmission error becomes larger for larger NAs. For hyper NA applications ($NA>1$), to achieve a dose variation smaller than $\pm 1\%$ requires a pellicle thickness variation of less than $\pm 1\text{-}2\text{nm}$.

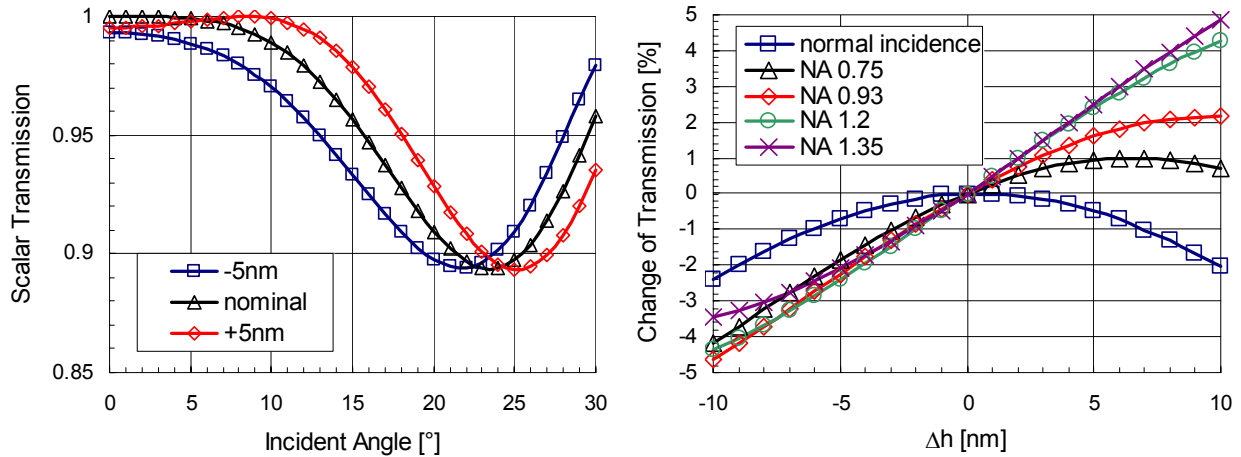


Figure 4: Left: scalar transmission vs. angle of incidence for varying film thickness $\Delta h = -5, 0, 5\text{nm}$; Right: transmission change at a pupil coordinate $0.9 \cdot NA$ vs. thickness change of pellicle for different NA's; pellicle parameter $n=1.4$, $h=828\text{nm}$.

Diattenuation

The pellicle-induced diattenuation for varying thicknesses is plotted in Fig. 5. Up to NAs of 0.93 the effect is rather small. However, for NA's larger than 1, diattenuation becomes quite significant, reaching values of around 2% for an NA of 1.35. When polarized light is used for imaging, the difference in both polarization states might change the intensity in the preferred state over the pupil. This is addressed in the next section.

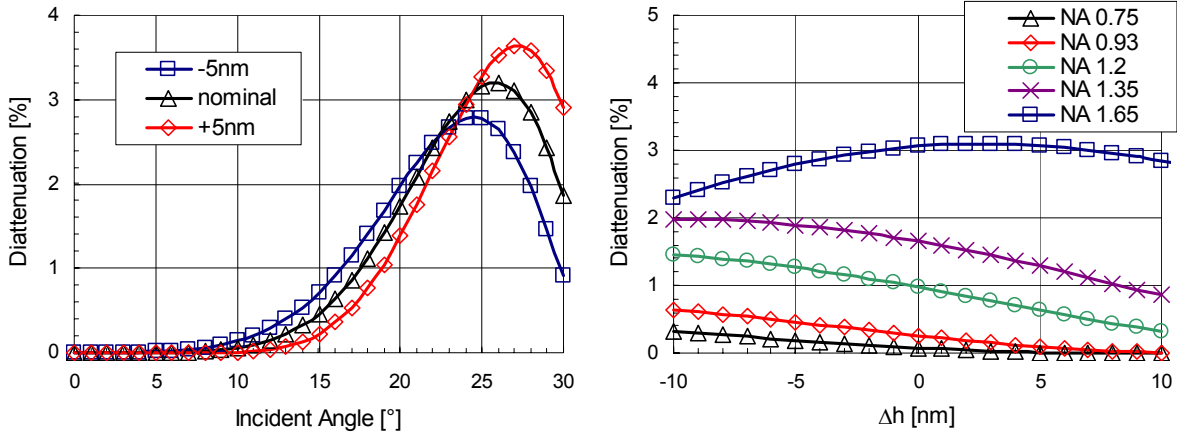


Figure 5: Left: pellicle induced diattenuation vs. angle of incidence for different thicknesses; Right: influence of varying pellicle thickness at the outer rim of the pupil for different NAs.

Scalar Phase

It is well known that a dielectric slab in the beam path of an optical system introduces spherical aberrations [11]. Whereas the lowest order term in the Zernike expansion Z4 can be compensated for by a focus shift, higher order Zernikes might be difficult to account for. Also, a change of best focus due to variation of the pellicle thickness might be a problem.

Spherical aberrations induced by the pellicle film are obtained from an expansion of the scalar phase in Zernike coefficients. We use the fringe Zernike polynomials and the SOLID-C numbering convention. A compensation of defocus Z4 at large NAs introduces higher order spherical aberrations [see, for example, 7]. In Fig. 6 the net spherical aberrations of the pellicle film are shown when defocus Z4 is cancelled out by a focus change (assuming an immersion liquid of $n=1.44$). For NAs smaller than 1, the higher order spherical aberrations are negligible. At an NA of 1.35 the Z9 value is around $-3m\lambda$ which is in the order of lens specifications. However, modern scanner can compensate for lowest order spherical aberration [7]. Higher order terms like Z16 are small up to NAs of 1.35.

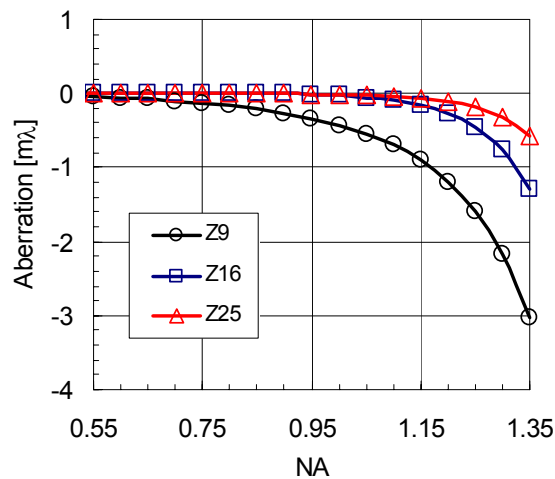


Figure 6: Pellicle induced spherical aberrations Z9, Z16 and Z25 vs. NA.

In Fig. 7, the change of spherical aberrations as a function of the film thickness is shown. Whereas for NAs smaller than 1, variations are small, Zernikes can differ in the range of a few $m\lambda$ for larger apertures. As an example we consider the case of an NA=1.35 with an immersion liquid $n=1.44$. The variation of Z4 for a film thickness change $\Delta h = \pm 10\text{nm}$ is approximately $4\ m\lambda$, which corresponds to a focus shift of around $\Delta z \approx 2\text{nm}$. For an NA of 1.65 under the assumption of a liquid with refractive index of $n=1.85$ we obtain similarly $\Delta z \approx 4\text{nm}$. Pellicle induced aberrations and their variations with membrane thickness are thus quite small.

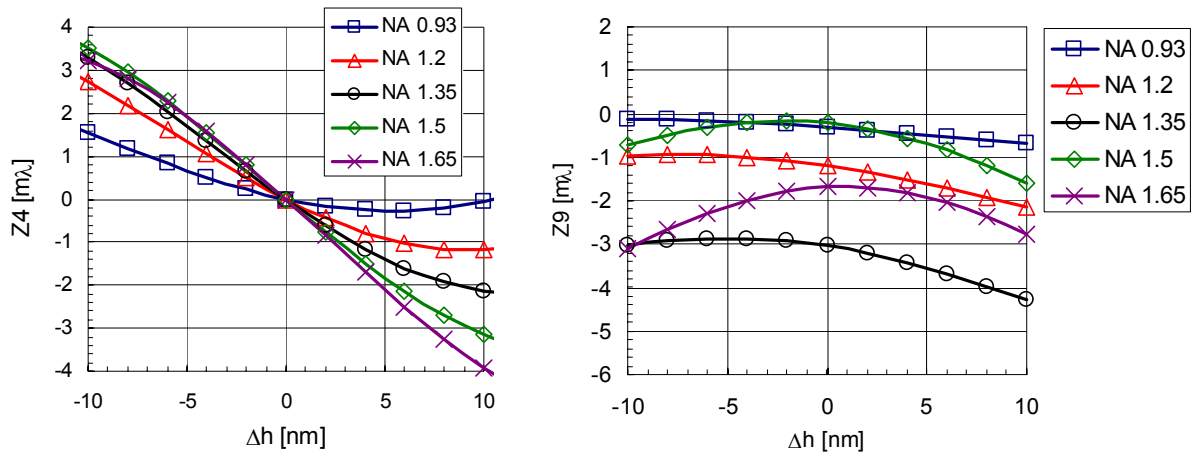


Figure 7: Left: change of defocus Z4 vs. pellicle film thickness; Right: higher order spherical aberration Z9 vs. membrane thickness; for $h=0$ defocus Z4 is compensated by shift of focal plane, immersion liquid with $n=1.44$ for NAs up to 1.35, $n=1.85$ for NA=1.5/1.65.

Retardance

Retardance describes the difference in phase between different polarization states. Causes for retardance can be intrinsic or stress induced birefringence. Whereas the polymer shows no intrinsic birefringence, stress in the film could in principle lead to birefringence. It was shown recently [6] that the pellicle has only a small influence on the net birefringence of a mask blank ($<1\text{nm/cm}$) indicating that this should not be an issue.

The effect investigated here is the retardance due to transmission through the film under large angles. A corresponding simulation is shown in Fig. 8. The retardance is smaller than 0.5° for NA's up to 1.65. A typical birefringence specification of $2\text{-}5\text{nm/cm}$ required for mask blanks corresponds to a phase difference of $0.3\text{-}0.9^\circ$ and is hence in the same order of magnitude. However, whereas substrate birefringence changes essentially the polarization state of the illuminator, the effect investigated here results in a change of polarization state over the pupil.

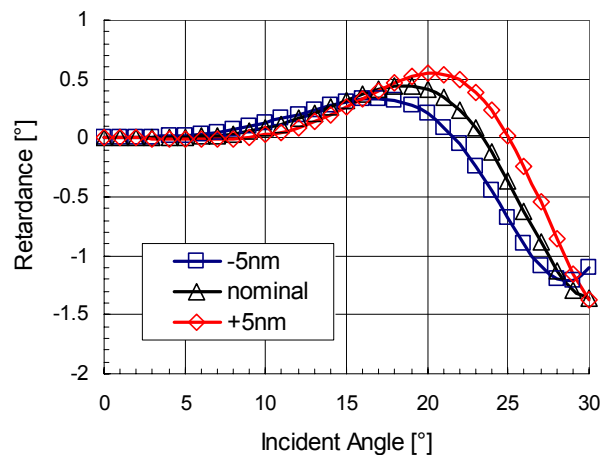


Figure 8: Pellicle induced retardance vs. angle of incidence.

For an investigation of the influence of pellicle induced transmission and phase on the lithographic performance it is desirable to describe the effects in a form which can be incorporated in lithography simulators. This can be done by using an effective Jones pupil which is the subject of the next section.

3. JONES PUPIL REPRESENTATION OF PELLICLE

A polarizing element without depolarization, i.e. the degree of polarization is retained, can be described in terms of Jones matrices [3,4]. For an optical system this means that the scalar pupil function describing wavefront aberrations and possibly apodization is replaced by a Jones pupil. Hence, every coordinate of the pupil is assigned to a Jones matrix which relates the polarization states at the entrance and exit pupil of the optical system. The net effect of a series of polarizing elements in the beam path can be obtained by matrix multiplication. The influence of the pellicle can thus be conveniently described with an additional Jones pupil.

As illustrated in Fig. 9, the Jones pupil of the pellicle film can be derived under the assumption of a possible tilt or bending of the membrane. These deformations are described as a change of the surface normal of the pellicle. The pellicle itself is assumed to be locally flat. That means, for a certain pupil (and object field) coordinate the local transmission of the pellicle depends on the mutual orientation of wavevector and surface normal of the pellicle film as written in Eqs. (1) and (2).

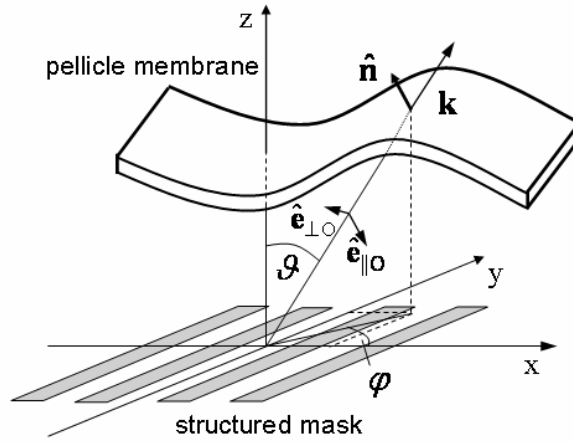


Figure 9: Sketch of underlying geometry.

As sketched in Fig. 9, an illuminating plane wave is diffracted by the structured surface of the mask in an angular spectrum of plane waves that propagate in different directions with wave vectors \mathbf{k} ,

$$\mathbf{k} = k_o \begin{bmatrix} p_{x_o} & p_{y_o} & \sqrt{1 - p_{x_o}^2 - p_{y_o}^2} \end{bmatrix}^T, \text{ with } p_x = \frac{p_{x_o}}{M}, p_y = \frac{p_{y_o}}{M} \text{ and } k_o = 2\pi/\lambda. \quad (7)$$

Here, p_{x_o} and p_{y_o} are the pupil coordinates in object space. The pupil coordinates in image space p_x and p_y are obtained by a scaling with the magnification factor M (here, $M=0.25$).

Before entering the entrance pupil of the lens, the respective waves need to pass the pellicle membrane where they experience a phase and transmission change according to Eq. (2). For a perfectly flat pellicle, which means that the surface normal \mathbf{n} is parallel to the optical axis ($\mathbf{e}_z = [0 \ 0 \ 1]^T$), the TE and TM components of the dielectric film coincide with the polarization states perpendicular to or in the meridional plane of the optical system, respectively. Here, the former is denoted by $\hat{\mathbf{e}}_{\perp O}$ and the latter by $\hat{\mathbf{e}}_{\parallel O}$ (see Fig. 3). The actual directions are,

$$\hat{\mathbf{e}}_{\perp O} = \frac{\hat{\mathbf{z}} \times \mathbf{k}}{|\hat{\mathbf{z}} \times \mathbf{k}|} \text{ and } \hat{\mathbf{e}}_{\parallel O} = \frac{\hat{\mathbf{e}}_{\perp O} \times \mathbf{k}}{|\hat{\mathbf{e}}_{\perp O} \times \mathbf{k}|}. \quad (8)$$

It is common to describe Jones pupils in terms of x and y linear polarization. Therefore, before application of Eq. (2), x and y linear polarization states need to be rotated into the TE and TM polarization state. The Jones pupil of the pellicle is hence given by,

$$\mathbf{J}_{\text{Pellicle}}(\mathbf{p}) = \mathbf{R}_1^{-1} \cdot \mathbf{F} \cdot \mathbf{R}_1, \quad (9)$$

where \mathbf{R}_1 describes the mapping of field vectors into the meridional plane of the optical system,

$$\begin{pmatrix} E_{\parallel O} \\ E_{\perp O} \end{pmatrix} = \mathbf{R}_1 \begin{pmatrix} E_x \\ E_y \end{pmatrix}, \text{ with } \mathbf{R}_1 = \frac{1}{\sqrt{p_x^2 + p_y^2}} \begin{bmatrix} p_x & p_y \\ -p_y & p_x \end{bmatrix}. \quad (10)$$

For a tilted or bent pellicle, the surface normal of the pellicle might be different at locations where a beam hits the membrane and is therefore dependent on the pupil coordinates. This requires an additional rotation from fields with directions $\hat{\mathbf{e}}_{\perp O}$ and $\hat{\mathbf{e}}_{\parallel O}$ into the eigenstates given in Eq. (1),

$$\mathbf{J}_{\text{Pellicle}}(\mathbf{p}) = \mathbf{R}_1^{-1} \cdot \mathbf{R}_2^{-1} \cdot \mathbf{F} \cdot \mathbf{R}_2 \cdot \mathbf{R}_1, \quad (11)$$

where \mathbf{R}_2 is given by,

$$\begin{pmatrix} E_{\parallel P} \\ E_{\perp P} \end{pmatrix} = \mathbf{R}_2 \begin{pmatrix} E_{\parallel O} \\ E_{\perp O} \end{pmatrix}, \text{ with } \mathbf{R}_2 = \begin{bmatrix} \cos(\phi_p) & \sin(\phi_p) \\ -\sin(\phi_p) & \cos(\phi_p) \end{bmatrix}, \cos(\phi_p) = \hat{\mathbf{e}}_{\perp O} \cdot \hat{\mathbf{e}}_{\perp P}. \quad (12)$$

The imaging equations normally used to describe a lithography system can now be extended to the case where the pellicle has a non negligible influence on the overall performance by an additional Jones element. The fields in resist due to a single source point with pupil coordinates \mathbf{a} can be written as (see, for example [3]),

$$\mathbf{E}(\mathbf{r}, \mathbf{a}) = \left| FT^{-1} \{ \boldsymbol{\psi}(\mathbf{p}) \mathbf{J}_{\text{Lens}}(\mathbf{p}) \mathbf{J}_{\text{Pellicle}}(\mathbf{p}) \mathbf{E}_{\text{Mask}}(\mathbf{a}, \mathbf{p}, \mathbf{E}_i) \} \right|^2, \quad (13)$$

where a Jones pupil describing the influence of the pellicle is added. \mathbf{E}_{Mask} is the diffracted vector field of the mask illuminated with a plane with polarization \mathbf{E}_i . \mathbf{J}_{lens} is the pupil coordinate dependent Jones matrix representation of the imaging lens. $\boldsymbol{\psi}$ describes vector effects and the polarization dependent incoupling in resist. FT^{-1} is the inverse Fourier transform which corresponds to the coherent interference of all fields due to a single source point. The image intensity is given by the incoherent superposition of fields resulting from an ensemble of source points $S(\mathbf{a})$,

$$I(\mathbf{r}) = \iint S(\mathbf{a}) \|\mathbf{E}(\mathbf{r}, \mathbf{a})\|^2 d^2 \mathbf{a}. \quad (14)$$

The impact of the pellicle film written in form of Eq. (11) can be incorporated in current lithography simulators. From Eq. (13) it becomes clear that the Jones pupil of the lens and the pellicle can be treated as one single element. It should be noted that in all simulations we assume a perfect lens, which means that \mathbf{J}_{lens} is the identity matrix. However, Jones pupils of both pellicle and lens might interact in a non trivial manner.

Fig. 10 shows the amplitude of the Jxx and Jxy components of a respective pupil for an NA=1.4. Polarization dependent apodization is shown in Jxx. Crosstalk between x- and y- polarization states due to diattenuation and retardance can be observed in the diagonal elements of Jxy. However, the actual transferred intensity between polarization states is small.

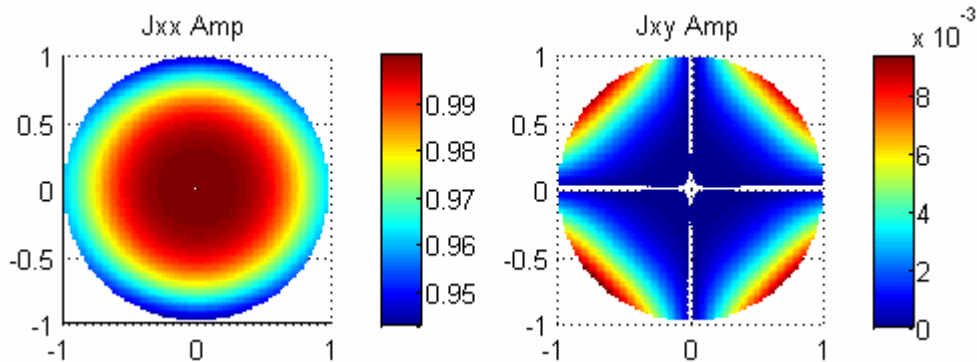


Figure 10: Jones pupil of pellicle for NA=1.4; only the amplitudes of Jxx and Jxy are shown.

4. INFLUENCE ON LITHOGRAPHIC PERFORMANCE

A complete investigation of possible implications of the effects described in Sections 2 and 3 is beyond the scope of this paper. However, in this section some simple examples are given which demonstrate the main impact of the presence of the pellicle membrane. These are dose variations due to thickness non uniformity and apodization. The discussion of the influence of the observed aberration levels as well as effects due to polarization dependent phase and transmission will be left for future investigation.

Dose Variation due to Thickness Non Uniformity

In a first step, an example of the influence of pellicle induced dose variations due to a variation of the film thickness is given. Here, the CD for 45nm and 65nm dense lines and spaces using a half-tone phase shifting mask is calculated. The simulations were performed using the optical lithography simulator ProlithTM (KLA Tencor). Effective Jones pupils for different pellicle membrane thicknesses were calculated according to Eq. (9) and imported into the simulator. The illumination is an azimuthally polarized quadrupole with opening angle 40° optimized at center partial coherence $\sigma_{\text{inner}}/\sigma_{\text{outer}} = 0.7/0.9$ at an NA=1.35 (45nm) and NA=0.93 (65nm). For a direct comparison of CD error, an index fluid with $n=1.44$ was assumed in both cases. In all simulations the image in resist is considered. A resist model might lead to an increase of the actual CD deviation. However, here we are interested in the order of magnitude of the effect.

The outcome of a corresponding simulation is shown in Fig. 11. For a pellicle thickness variation of $\pm 5\text{nm}$ a CD variation up to 6% for 45nm half pitch is obtained. As an azimuthal polarization is chosen here, the effect observed is due to the change in transmission through the pellicle membrane. This is also evident from a direct comparison of Fig. 11 with Fig. 4. The results shown here imply the necessity of tight specifications on film thickness.

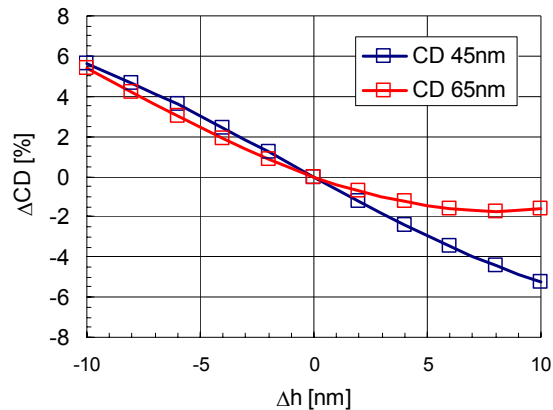


Figure 11: CD variation vs. pellicle thickness for 45nm (NA=1.35) and 65nm (NA=0.93) dense lines and spaces.

Influence of Apodization on OPC

As the apodization described in Sections 2 and 3 acts as an effective pupil filter, it will have an impact for example, on OPC. This is demonstrated by means of a simple OPC simulation for through pitch imaging of semi dense lines with target CDs of 45 and 40nm, respectively. The simulation parameters are given in the caption of Fig. 12. The threshold is fixed for 40/45nm 1:1 dense lines and spaces. For every pitch we calculate the line width for which the target CD is obtained. No assist features are considered in the simulation.

Fig. 12(a) shows a plot of the required linewidth to print the nominal linewidth (40nm or 45nm) through pitch calculated without pellicle. With pellicle apodization, the diffraction orders are weighted depending on their location in the pupil, which in return has an influence on OPC. This is illustrated in Fig. 12(b), where the difference in required linewidth with and without the pellicle membrane is plotted. The deviations can be as large as 4nm on the mask, which is in the order of off-target CD specifications at these small nodes. Large differences are observed where diffraction orders move along the outer rim of the pupil. The differences increase for smaller nodes. In a further simulation the CD error with pellicle was calculated for OPC performed without a pellicle. The result of a corresponding simulation is shown in Fig 12(c). CD errors can be as large as 2% for 40nm halfpitch. This indicates the necessity of incorporating pellicle induced apodization for OPC.

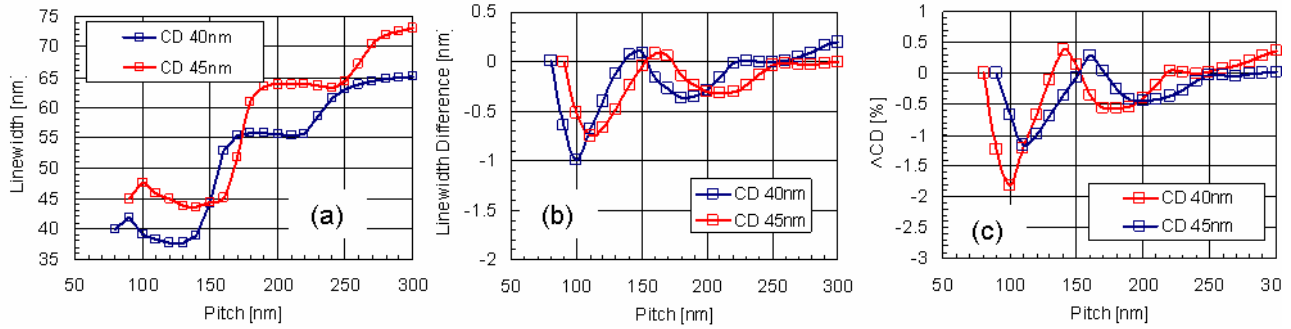


Figure 12: (a) Required linewidth after OPC for through pitch imaging for target CDs 40 and 45nm calculated without pellicle, all values are given in wafer scale; (b) Difference of required linewidth calculated with and without pellicle; (c) CD error for through pitch imaging due to pellicle for OPC curve calculated without pellicle; Parameter: NA=1.35/1.2 for 40nm/45nm halfpitch, DipoleX, $\sigma=0.79/0.99$, 40° opening angle, TE/y-polarization, image in resist n=1.7, immersion liquid n=1.44.

5. INFLUENCE OF A BOWED PELLICLE FRAME

It is well known that a tilted plane parallel plate introduced in the beam path of an optical system gives rise to displacement errors [11]. This might be an additional effect to the well investigated in-plane distortions induced on optical photomasks by bonding of a non perfect pellicle frame [12].

Whereas a global tilt of the pellicle film can be adjusted for by the scanner, a local tilt or a more complicated height variation of the pellicle film is difficult to compensate for. For the application of hard pellicles a tight specification for local tilt of around 10 μ rad was required to reduce displacement errors below 1nm [7]. As the soft pellicle considered here is much thinner, the induced displacement due to a given tilt is also much smaller. However, it is known that pellicle frames can have a considerable frame bow with varying curvatures [12,13]. As the thin polymer membrane is stretched over the frame, considerable local tilts are expected. The height variation of the frame is reduced when the pellicle is attached to the reticle. However, the adhesive between frame and membrane might also show height variations in the order of tenths of microns. It is therefore necessary to investigate the possible influence of a bowed pellicle membrane.

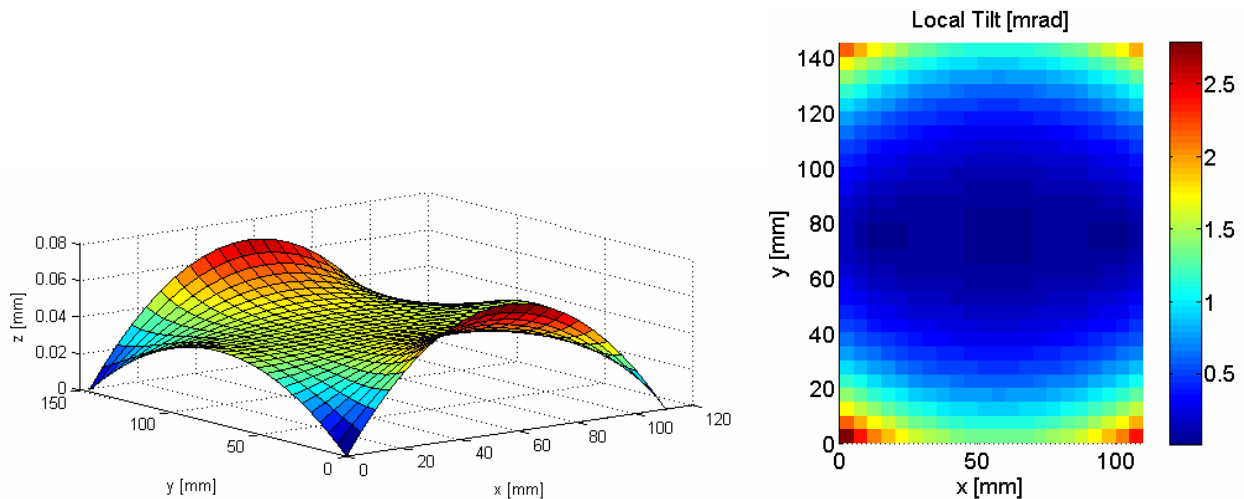


Figure 13: Left: simulated example of pellicle topography with maximum overall bow of 70 μ m; Right: corresponding plot of local tilt.

The height topography $h(x,y)$ of a pellicle film suspended over a frame with a certain frame shape can be described by Poisson's equation,

$$\frac{\partial^2 h(x,y)}{\partial x^2} + \frac{\partial^2 h(x,y)}{\partial y^2} - g = 0 \quad (15)$$

where a parameter g is included to describe the action of gravity. However, simulations indicated that in our case gravity can be neglected. The solution to Poisson's equation is uniquely determined by the value of the function specified on all boundaries, meaning in our case the frame curvature. Eq. (15) can be solved, for example, with a finite difference scheme. A simulation of the film topography for a pellicle frame with an overall bow of $70\mu\text{m}$ and a map with the corresponding local tilt is shown in Fig. 13. The local tilt due to distortions is usually in the order of 0.5-2 mrad for typical frame curvatures.

The Jones pupil for a given field point on the mask can, in principle, be calculated as follows. First, the topography $h(x,y)$ for a given frame curvature is calculated as described above. For a given pupil coordinate and hence an associated wave vector the coordinate where the beam hits the pellicle can be determined. The Jones matrix at this particular location in the pupil is then given by the angle between wave vector \mathbf{k} and surface normal \mathbf{n} according to Eq. (12). However, for a slowly varying height of the pellicle membrane the surface normal of the film can be assumed to be constant for a given field point. Simulations showed that this is indeed the case for realistic frame curvatures.

In Fig. (14), aberrations for a given tilt around the y-axis are shown. The predominant aberration is clearly x-tilt Z2. The contribution of pellicle tilt to x-coma Z7 is rather small. As already mentioned, a tilt will lead to displacement errors. This is shown in the left plot of Fig. 14, where displacement of dense lines and spaces with illumination settings as described in Section 4 is depicted. Here, Jones pupils according to Eq. (11) were calculated and used in the simulations. The actual values are in good agreement with approximate formulae given in the literature [7]. Even for large height deviations of the frame in the order of $100\text{-}200\mu\text{m}$ or for a more complicated frame curvature than shown in Fig. 12 the local tilt should not exceed 5mrad. The resulting displacement is well below 1nm.

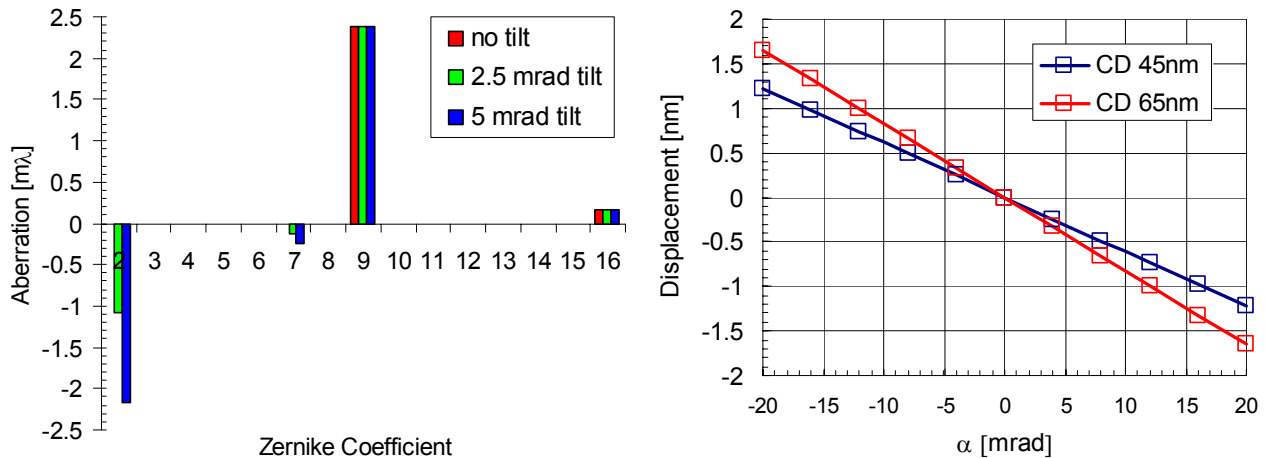


Figure 14: Left: Scalar aberrations for varying local tilt of pellicle (not shown is defocus Z4); Right: Displacement versus pellicle tilt; same parameter as in Fig. 11.

A tilt of the pellicle frame leads also to a shift of the apodization in the pupil. In principle, this changes the weighting of diffraction orders which in return can, for example, introduce CD errors. However, simulations using Jones pupils based on Eq. (12) showed that CD errors are less than a tenth of a nm. This suggests that a bowed pellicle film has only minor influence on lithographic performance.

6. CONCLUSIONS

For large angles of incidence as occurring in Hyper NA systems, common pellicle membranes show a significant radial apodization. The transmission can drop of around 10% near the rim of the pupil. More importantly, the change in transmission for varying pellicle thickness increases dramatically. As the dose variations vary across the pupil, their influence is structure dependent and might be difficult to compensate for with, for example, dose mapping schemes. Higher order spherical aberrations are in the order of some $m\lambda$. Also, a significant diattenuation of around 2-3% can be observed. The pellicle induced retardance at large angles is in the same order of magnitude as mask blank birefringence values required for applications with polarized light.

The action of the pellicle can be described by an effective Jones pupil. Simulations showed a significant impact of pellicle thickness on wafer CD. The apodization of the pellicle needs to be taken into account for correct OPC. The effect of a bowed pellicle due to a non perfect frame bow on displacement and CD is small.

The results presented confirm the need to check if current pellicles are suitable for Hyper NA applications. Without modifications, the film thickness specifications should be in the order of $\pm 1-2$ nm. To prevent large apodization close to the rim of the pupil, anti reflective coatings or lower refractive index materials are necessary.

ACKNOWLEDGEMENTS

AMTC is a joint venture of Infineon, AMD and Toppan Photomasks and gratefully acknowledges the financial support by the German Federal Ministry of Education and Research (BMBF) under Contract No. 01M3154A (“Abbildungsmethodiken für nanoelektronische Bauelemente”). We thank Andreas Erdmann from Fraunhofer IISB Erlangen and Ralf Ziebold from Infineon Technologies for useful discussions.

REFERENCES

1. D. G. Flagello, S. Hansen, B. Geh, and M. Totzeck, „Challenges with Hyper-NA (NA>1.0) Polarized Light Lithography for Sub $\lambda/4$ resolution“, *Proceedings of the SPIE*, vol. 5754, pp. 53-68, 2005.
2. G. E. Bailey, Kostas Adam, „Polarization influences through the optical path“, *Proceedings of the SPIE*, vol. 5754, pp. 1102-1112, 2005.
3. M. Totzeck, et al, “How to describe polarization influence on imaging”, *Proceedings of the SPIE*, vol. 5754, pp. 23-37, 2005.
4. J. Kye, et al, “Polarization aberration analysis in optical lithography systems”, *Proceedings of the SPIE*, vol. 6154, 2006.
5. B. Geh, et al, “The impact of mask birefringence on hyper-NA (NA>1.0) polarized imaging”, *Proceedings of the SPIE*, vol. 5992, pp. 317-331, 2005.
6. A. Estroff, Y. Fan, A. Bourov, B. W. Smith, „Mask-induced polarization effects at high numerical aperture”, *JM3 - Journal of Microlithography, Microfabrication, and Microsystems* 04 (03), 2005.
7. P. D. Bisshop, “Initial assessment of the impact of a hard pellicle on imaging using a 193nm step-and-scan system”, *JM3 - Journal of Microlithography, Microfabrication, and Microsystems* 03 (02), pp. 239-262, 2004.
8. W.-H. Cheng, “Vectorial effects in subwavelength mask imaging”, *Proceedings of the SPIE*, vol. 5992, pp. 397-407, 2005.
9. F. Eschbach, et al, “Photomask lifetime issues in ArF lithography”, *Proceedings of the SPIE*, vol. 5853, pp. 74-82, 2005.
10. M. Born and E. Wolf, “Principles of Optics”, Cambridge University Press, Cambridge, 2003.
11. W.J. Smith, “Modern Optical Engineering-The Design of Optical Systems”, McGraw-Hill, 1990.
12. E. Cotte, et al, “Effects of soft pellicle frame curvature and mounting process on pellicle-induced distortions in advanced photomasks”, *Proceedings of the SPIE*, vol. 5040, p. 1044-1054, 2003.
13. E. Cotte, “Numerical and experimental analysis of pellicle induced distortions of photomasks”, PhD thesis, University of Wisconsin-Madison, 2001.
14. J. S. Gordon, “Pellicles designed for high performance lithographic process”, *Proceedings of the SPIE*, vol. 2512, pp. 99-111, 1995.